From SWIRLS to RAPIDS : Nowcast Applications Development in Hong Kong

M.C. Wong, W.K. Wong, and Edwin S.T. Lai
Hong Kong Observatory
Hong Kong, China

1. INTRODUCTION

The Hong Kong Observatory started a programme to develop a rainstorm nowcasting system SWIRLS (Short-range Warning of Intense Rainstorms in Localized Systems) in 1997. A SWIRLS prototype was put on operational trial in the rain season of 1998. The pilot experiment was considered to be a success with quantitative rainfall forecasts in the first couple of hours proving especially popular as an additional reference material for forecasters in operating the Rainstorm Warning System. Following some minor revisions based on users' input, SWIRLS was officially declared operational in April 1999.

The key development objective in SWIRLS is to make use of both radar and raingauge data to monitor and predict local rainfall distribution trends within the next couple of hours. The combined re-analyzed data set, based on a time-adjusted reflectivity-rainfall relationship, has proved to be extremely useful for provision of real-time rainfall information to the public and government decision-makers, formulation of nowcasting strategies, as well as for physical initialization in numerical weather prediction.

The main algorithms developed, namely TREC (Tracking Radar Echoes by Correlation) and Quantitative Precipitation Forecast (QPF), are presented in this paper. Other supporting SWIRLS applications, e.g. TephiViewer and GTrack, are also introduced in brief. The paper also includes a glimpse into the future, highlighting the development of RAPIDS (Rainstorm Analysis & Prediction Integrated Data-processing System) in an effort to extend QPF capability through the blending of SWIRLS and NWP output.

2. ECHO MOVEMENT AND TREC

Movement of individual radar echo between two consecutive CAPPI scans at 6-minute interval is derived using the TREC correlation method. Cross-correlation technique was first used to determine the movement of the entire storm cluster (Hilst and Russo [1]; Kessler and Russo [2]; Crane [3]; Bjerkaas and Forsyth [4]). With the availability of higher resolution radar data, this technique was extended to retrieve the individual motion vectors of embedded storm cells (Rinehart and Garvey [5]; Rinehart [6]; Smythe and Zrnic [7]; Tuttle and Foote [8]).

The main advantage of using correlation method is that it requires only information from one single radar at two different observation times. Although the derived motion field is essentially two-dimensional in the horizontal and does not include strong vertical motion normally expected in convective cloud systems, the approximation should be good enough given that the effect of horizontal advection should be more pronounced if only short-term motion is considered. Once the motion vectors are computed, the entire echo field can be extrapolated to produce a short-term (say, one-hour) forecast field.

TREC method is applied to two successive CAPPI reflectivity fields 6-minutes aparts. The first field (at time T_1) is divided into a number of equally sized "boxes" or two-dimensional arrays of pixels. The arrays of reflectivity values will then be cross-correlated with the arrays in the second field (at time $T_2 = T_1 + 6$ minutes). Computation can be repeated for all possible arrays found at T_2 to determine which array results in the highest correlation, and the centre of this second array will be the end point of the motion vector (i.e. TREC vector). In practice, to reduce computation time, a search area centred on the first array is prescribed (Figure 1).

According to Tuttle and Foote [8], the size of the "boxes" should be bounded by two considerations. A small "box" will contain too few data points for the correlation coefficients to be stable. A large "box" will only give the general mean flow on a broad spatial scale. In our study, the reflectivity field has a resolution of 480×480 pixels and the standard ranges of radar scan vary from 64 km, 128 km to 256 km. The array is set to have a fixed size of 19×19 pixels and thus the array size varies from 5 km (for 64km range of scan) to 20 km (for 256 km range of scan). The centres of pixel arrays are spaced 5 pixels apart and the whole TREC vector field has a resolution of 93×93. The search radius, which determines the expected maximum velocity of the echo motion, is usually set to be about the box width or it can be set according to sounding information.

Before the whole vector field is analyzed objectively, each motion vector has to pass a preliminary consistency check. If a TREC vector deviates more than 25 degree from the local mean of its neighbourhood (which is calculated from the set of 25 vectors located around it), it will be replaced by this mean vector. In this way, the "noisiness" as a result of sole consideration of maximum correlation in deriving the motion vector can be reduced at an early stage. To produce a continuous gridded vector field, a three-pass objective analysis using modified Cressman weighting function is then applied (Cressman [9]).

Objective analysis is performed separately for the two components of the TREC vector field. The radius of influence can be set to arbitrary values in the three passes. For the TREC vector field of resolution 93×93, the radius is set at 31 pixels, 16 pixels and 8 pixels for the first, second, and third pass respectively. This set of decreasing radius values is found to be most applicable in retaining the main features while giving a smooth and continuous field of TREC vectors on output.

The forecast radar reflectivity pattern is obtained by extrapolation based on the smoothed TREC vectors. Temporal integration makes use of the two-time-level semi-Lagrangian scheme (Staniforth and Cote [10]). As the vector field is computed from consecutive radar CAPPI images six minutes apart, the integration scheme can output forecasts in 6-minute interval, and each successive forecast pattern is then used for the next step of integration.

Results from recent studies show that TREC is able to reproduce realistic wind fields associated with major weather systems. For example, the perturbed flow in the westerlies was well depicted in the travelling squall line on 2 May 1998 (Figure 2). For two typhoons that passed over Hong Kong on 2 August 1997 (Victor) and 7 June 1999 (Maggie), their wind circulations and asymmetric structures were both captured by TREC (Figures 3 and 4).

3. RAINFALL RE-ANALYSIS AND FORECAST

Apart from tracking the echoes and making a good short-range projection in movement and intensity, the amount of rain received at the surface remains the main forecasting issue. Conventionally, the Marshall-Palmer relationship is used in converting echo intensity (i.e. reflectivity, Z) to rainfall, R. But it is well known that the relationship is too generalized and does not apply well in many cases. To obtain a better estimate, SWIRLS makes use of raingauge data over Hong Kong to calibrate radar reflectivity in real time. In other words, the Z-R relationship will be adjusted in time as the rain event unfolds. If rain has not fallen as yet over any of the gauges and hence no ground truth available, the latest Z-R relationship from the last rain episode will be used as first guess.

To optimize the parameters a and b in the conventional $Z=aR^b$ relationship, radar reflectivity is correlated every five minutes with the rainfall recorded by the raingauges underneath. The adjusted Z-R relationship is used subsequently in the forecast module, based on TREC winds, to convert the forecast radar reflectivity into rainfall over the raingauge positions (Figure 5).

Various factors can affect the accuracy of the radar-rainfall estimation. Some of these factors are inherent in the radar beam characteristics and cannot be readily rectified. However, some studies such as Zawadzki *et al.* [11] also suggest that sufficient accuracy in radar-rainfall estimation within a short distance (say, within 30 km from the radar) can still be achieved through a suitable choice of spatial and temporal resolution in the calculation. Based on the Zawadzki paper, the following procedure is adopted to adjust the Z-R relationship (Figure 6).

Radar CAPPI reflectivity images at 1-km height are used for the correlation exercise. The low altitude is chosen to be as close to the cloud base as practicable and hence more likely for the raindrops to preserve their volume on reaching the ground. Radar reflectivity data on polar coordinates are then converted into Cartesian coordinates for co-locations with the raingauge positions. Due to the presence of winds, falling raindrops will deviate horizontally from their starting positions. A search area from each raingauge position can be empirically adjusted to take this effect into account. Operationally, the default search area is defined to be within a distance of one pixel, i.e. over a 3 x 3 grid. The maximum intensity value within the search area, rather than intensity value averaged over the search area which is found to be less effective from investigative experiments, is assigned to the raingauge to form a potential radar-raingauge pair. An interpolation algorithm is also implemented to deal with the non-synchronous problem arising from the 6-minute radar volume scans and the 5-minute surface rainfall data measured by the tele-communicating automatic raingauges distributed over Hong Kong.

After some basic quality checks, the radar-raingauge pairs are passed to a linear least square analysis for the determination of a and b, i.e.

$$\mathrm{dBZ} = 10 \log a + b\ \mathrm{dBG}$$

where dBG is the raingauge rainfall expressed in decibel. To ensure statistical significance, all reporting radar-raingauge pairs, once accepted, will be retained for the linear least square analysis throughout the entire rain episode. Any departure of more than 2 standard deviation units from the best fit line will be discarded and the correlation will be re-calculated until a correlation coefficient of $r \geqq 0.7$ is reached. Results have proven that the adopted approach is

able to obtain reasonable Z-R relationship (Figure 7).

When there are not enough reporting radar-raingauge pairs, such as when a rainstorm is still outside Hong Kong, either the standard Marshall-Palmer relationship (a = 200, b = 1.6) or the Z-R relationship from the previous rain episode will be used. As more radar-raingauge pairs become available, the Z-R relationship will be updated accordingly.

Echo intensity change is a result of many complex processes and close monitoring of echo development is essential for successful nowcasting. The TREC winds provide a basis to estimate the extent of growth and decay associated with each echo pixel. As the TREC vector traces the trajectory of individual echo, the difference in echo intensity along the flow between two successive radar scans can also be deduced. This information can be suitably included in the forecast if so desired. Keeping things relatively simple to start with, there are several possibilities in estimating short-term echo intensity changes: (a) assuming no change as from the latest scan; (b) assuming linear extrapolation from the latest scans; (c) imposing an idealized intensity profile upon the intensity trends as observed from the latest scans. In SWIRLS, option (a), i.e. no echo development, is often used as reference for both 1-hour and 2-hour rainfall forecasts. It may seem too simplistic but given the complexity of the problem, it has the advantage of providing forecasts with good continuity when the advective process dominates (such as in the cases of tropical cyclone rainbands shown in Figures 8 and 9), or even reasonable qualitative estimates and categorical forecasts for rainstorm warning operation in cases of significant echo intensity changes should rain generation and degeneration balance out on the broader scale.

4. OTHER SWIRLS PRODUCTS

Two other applications, namely GTrack and TephiViewer, are also made available in SWIRLS to assist forecasters in assessing potential or developing rainstorm scenarios.

GTrack

GTrack (Group Tracking) is another echo movement module to complement TREC for a more complete description of echo motion. With suitably chosen box size, the TREC module can reveal the motion of echoes on different spatial scales, including the inner structure of the target rainstorm. GTrack, on the other hand, groups the pixels over some pre-defined intensity threshold in the form of an ellipse and tracks the movement of ellipse centroids between successive radar images. In other words, GTrack is an “object-oriented” technique for tracking the movement of a storm as a whole entity. Extension of the TREC technique to group tracking of echoes (i.e. GTrack) have enabled forecasters to make qualitative educated guess on the likelihood of prolonged heavy rain or the potential of enhanced storm development (Figure 10).

For GTrack QPF, the adjusted Z-R relation analyzed in TREC is used to convert the reflectivity values enclosed within an ellipse into rainfall rates. Based on the distribution of the pixel values within the cell, a number of rainfall quantities can be derived, including maximum, minimum, meanal, and total accumulated rainfall estimation associated with and during the projected passages of the ellipses. For ellipses that have hourly rain rates over certain warning thresholds (e.g. 30, 50 or 70 mm/hr), special symbols will be superimposed on the cells to alert the forecasters on the possibility of heavy rain. Users are also provided with options to choose what thresholds they would like to use so as to focus on systems of different intensity levels.

TephiViewer

There are two streams of products within the TephiViewer. A collection of often used instability indices, including actual observations as analyzed from soundings and predicted values as deduced from NWP models, are displayed in time series for forecasters' reference. Forecasters can, at a glance, assess the prevailing trends in atmospheric stability, as well as compare predicted figures against actual observations to evaluate model performance and reliability. In the tephigram plotting of the latest soundings, forecasters can interactively adjust the temperature and dew point profiles by clicking and dragging at the observation points. The corresponding instability indices will be automatically updated and displayed at the same time, thereby providing an indication on the overall effect such adjustments have on atmospheric stability. The idea is that through such man-machine interaction, the atmosphere's sensitivity to probable changes, either as suggested by real-time near-surface observations or as implied by NWP models, and hence the risks of convection triggering can be more effectively monitored.

5. RAPIDS – BLENDING SWIRLS AND NWP OUTPUT

SWIRLS has been operating since 1999 to provide the quantitative precipitation forecast (QPF) up to 3 hours ahead. Verification results (Wong et al. [12]) show that the SWIRLS QPF is skillful for the nowcasting of rainstorm in the next one to two hours, especially the situations where the advection of precipitation system is dominant. When the rainstorm motion is erratic or when echoes develop or dissipate rapidly, advection methods are less reliable and more sophisticated forecasting techniques like high resolution numerical weather prediction (NWP) models are necessary, especially in the forecast range beyond 2-3 hours. On the other hand, NWP models usually suffer from the intrinsic "spin-up'' problem, hence hindering reliability of numerical prognoses in the first couple of hours. To achieve an optimal performance in the 1 to 6 hours range, HKO is developing a new nowcasting rainstorm forecasting system called RAPIDS (Rainstorm Analysis & Prediction Integrated Data-processing System) incorporating the best features of SWIRLS and NWP forecasts. The goal of RAPIDS is to blend or merge the SWIRLS with NWP to generate an optimal QPF for operational guidance in rainstorm situations. The first version of RAPIDS has been put in trial run since April 2005 to provide an hourly update QPF for the next 6 hours at horizontal resolution of 2 km. RAPIDS consists of 3 components: (a) SWIRLS QPF, (b) QPF from the HKO Non-hydrostatic Model (NHM) and (c) the blending algorithm (Figure 11).

The NWP component employed in RAPIDS is the Non-hydrostatic Model (NHM) adapted from the Japan Meteorological Agency (Saito et al. [13]). HKO has started trial operation of NHM since April 2004 to provide short-range QPF guidance to forecasters. The horizontal resolution is 5 km with 45 terrain-following vertical levels, with a model domain covering 600 x 600 km^2 of areas centred over Hong Kong. The initial and boundary fields are obtained from the Hong Kong Observatory's 20-km Regional Spectral Model (RSM).

To tackle the problem of observed errors in space, time and intensity in the model rainfall forecast, a phase correction is developed and applied to NHM QPF before the rainfall fields are merged with the SWIRLS output. Departures in the forecast precipitation patterns from NHM output in location are estimated with respect to the actual radar-rainfall distribution (i.e. radar-estimated rainfall calibrated against rain-gauges). The phase correction to eliminate spatial misfit is determined by an optimal transformation which minimizes the square error of the

forecast rainfall field and the actual rainfall distribution. A gross optimal spatial translation is determined either from phase-correlation motion techniques using 2-D Fourier transform or variational technique. Further adjustments in shape and orientation of rainfall patterns are carried out either in projective or shape-preserved 2-D rigid transformation (Szeliski [14]). An example on phase adjustment of NHM QPF towards the actual rainfall pattern and the resultant RAPIDS QPF for a rainstorm case on 2 June 2006 is illustrated in Fig. 12.

RAPIDS, incorporating QPF from SWIRLS advection-based nowcasting techniques and NHM, is currently under trial operation at HKO. The new system aims to combine the skills of SWIRLS and NHM QPF through an optimal blending scheme. More weights are assigned to SWIRLS QPF in the first couple of hours, with NHM input increasing in importance in the latter part of the 6-hour forecast range. The temporal variation of blending weights of adjusted NHM QPF is given in Fig. 13, in which the lower and upper boundaries of weighting (α and β) are tunable parameters, computed in real time by validating the actual performance of SWIRLS and NHM QPF as the rain event unfolds.

Case study and verification results reveal that the performance of RAPIDS in short-range forecast of precipitation is generally satisfactory, making it a feasible approach to extend the skill of operational forecast of rainstorm beyond the first three hours. Fig. 14 shows verification results of performance of RAPIDS, NHM and SWIRLS during May to August in 2005. About 170 forecast cases are verified and rain/no rain criteria (using threshold at 1 mm/hr) is used. It can be observed that the RAPIDS has a higher probability of detection (POD) than both SWIRLS and NHM through the blending of the two QPFs. At the same time, RAPIDS has a smaller false alarm ratio (FAR) than NHM DMO (Direct Model Output), but remains higher than that of SWIRLS QPF in the first 4 hours of forecast.

6. FUTURE DEVELOPMENT OF SWIRLS AND RAPIDS

SWIRLS is currently undergoing an enhancement process to incorporate more nowcasting capability in the prediction of severe weather phenomena associated with rainstorms, e.g. lightning, severe thunderstorms/hailstorms, and squalls. The algorithms and applications developed will be tested out through the WMO/WWRP Beijing 2008 Forecast Demonstration Project (B08FDP).

Planned enhancements of RAPIDS are aimed at reducing the false alarm ratio by tuning the phase correction schemes using constraints imposed by parameters derived from NHM forecasts, such as stability conditions and diagnosis of governing factors on heavy rain and severe weather. This will be done in parallel with continuing development associated with NHM, particularly in terms of refinement in model resolution, extension of NHM domain, ingestion of more moisture-related data and assimilation of non-conventional data through variational techniques. Possibility to include information on the echo growth and decay processes in SWIRLS will also be explored. The use of hourly-updated NHM will also create an opportunity for the development of probabilistic QPF product using time-lagged ensemble techniques.

REFERENCES

[1] Hilst, G.R., and J.A. Russo, Jr., 1960: An objective extrapolation technique for semi-conservative fields with an application to radar patterns. Tech. Memo. No. 3, Travelers Weather Research Centre, Hartford, CT.

[2] Kessler, E., III, and J.A. Russo, Jr., 1963: Statistical properties of weather echoes, *Preprints 10th Weather Radar Conf.,* Washington, DC, Amer. Meteor. Soc., 25-33.

[3] Crane, R.K., 1979: Automatic cell detection and tracking. *IEEE Trans. Geosci.Electron.*, **GE-17**, 250-262.

[4] Bjerkaas, C.L., and D.E. Forsyth, 1980: Operational test of a three-dimensional echo tracking program. *Preprints 19th Conf. Radar Meteorology* Miami Beach, Amer. Meteor. Soc., 244-247.

[5] Rinehart, R.E., and E.T. Garvey, 1978: Three-dimensional storm motion detection by conventional weather radar. *Nature,* **273,** 287-289.

[6] Rinehart, R.E., 1979: Internal storm motions from a single non-Doppler weather radar. NCAR/TN-146+STR, 262pp.

[7] Smythe, G.R. and D.S. Zrnic, 1983: Correlation analysis of Doppler radar data and retrieval of the horizontal wind. *J. Climate and Appl. Meteor.*, **22**, 297-311.

[8] Tuttle, J.D. and G.B. Foote, 1990: Determination of the Boundary Layer Airflow from a Single Doppler Radar. *J. Atmos. Ocean. Tech.,* **7**, 218-232.

[9] Cressman, G.P., 1959: An operational objective analysis system. *Mon. Wea. Rev.,* **87**, 367-374.

[10] Staniforth, A. and J. Cote, 1991: Semi-Lagrangian integration schemes for atmospheric models – a review. *Mon. Wea. Rev.*, **119**, 2206-2223.

[11] Zawadzki, I., C. Desrochers & E. Torlaschi, 1986: A Radar-raingauge Comparison. Preprints, *23rd Conf. on Radar Meteorology*, Snowmass, Colorado, Amer. Meteor. Soc., 121-124.

[12] M.C. Wong, E.S.T. Lai & P.W. Li, 2006: Application of Nowcast Products to Real-time Warning of Hazadous Weather in Hong Kong. *PWS Worskhop on Warnings of Real-Time Hazards by Using Nowcasting Technology*, Sydney, Australia, 9-13 October 2006.

[13] Saito, K., T. Fujita, Y. Yamada, J. Ishida, Y. Kumagai, K. Aranami, S. Ohmori, R. Nagasawa, S. Kumagai, C. Muroi, T. Kato, H. Eito and Y. Yamazaki, 2006: The operational JMA nonhydrostatic mesoscale model. *Mon. Wea. Rev.*, **134**, 1266-1298.

[14] Szeliski R., 1996: Video mosaics for virtual environments. *IEEE Computer Graphics and Applications*, **16(2)**, 22-30.

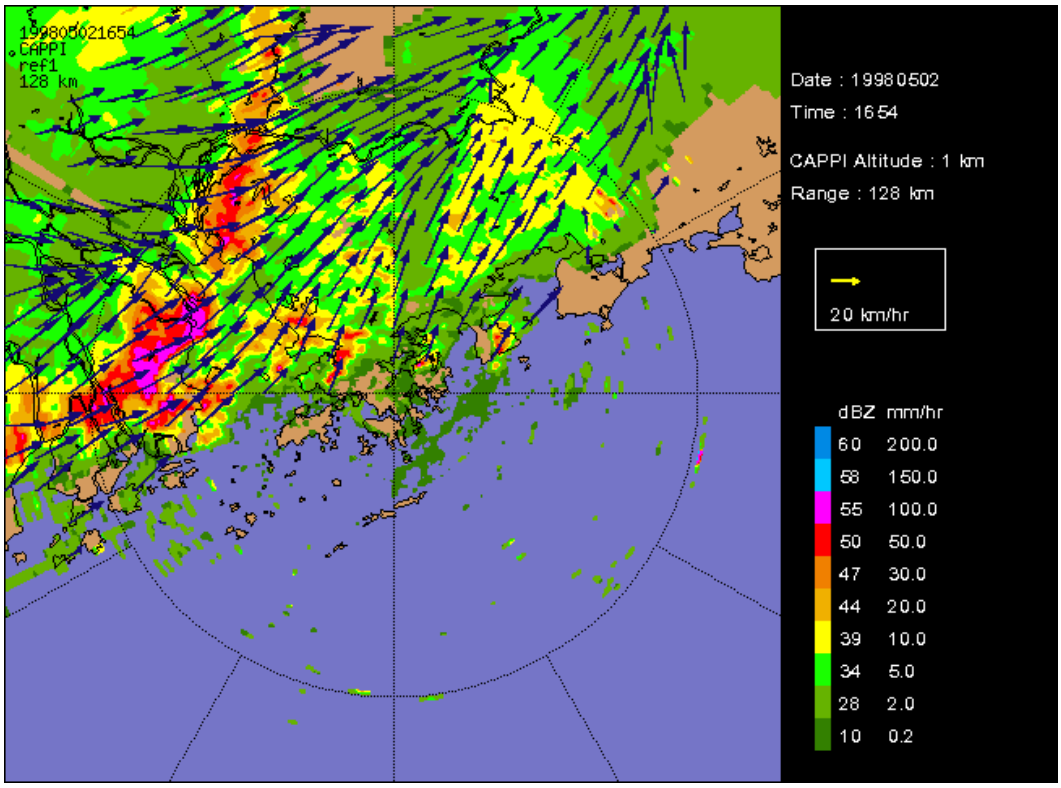

Figure 1 Schematic diagram showing the computation of the TREC vector to find the motion of reflectivity echoes (shaded). The pixel array at Time 1 is

Figure 2 TREC analysis of a squall line approaching Hong Kong from the northwest at 15:54 HKT on 2 May 1998.

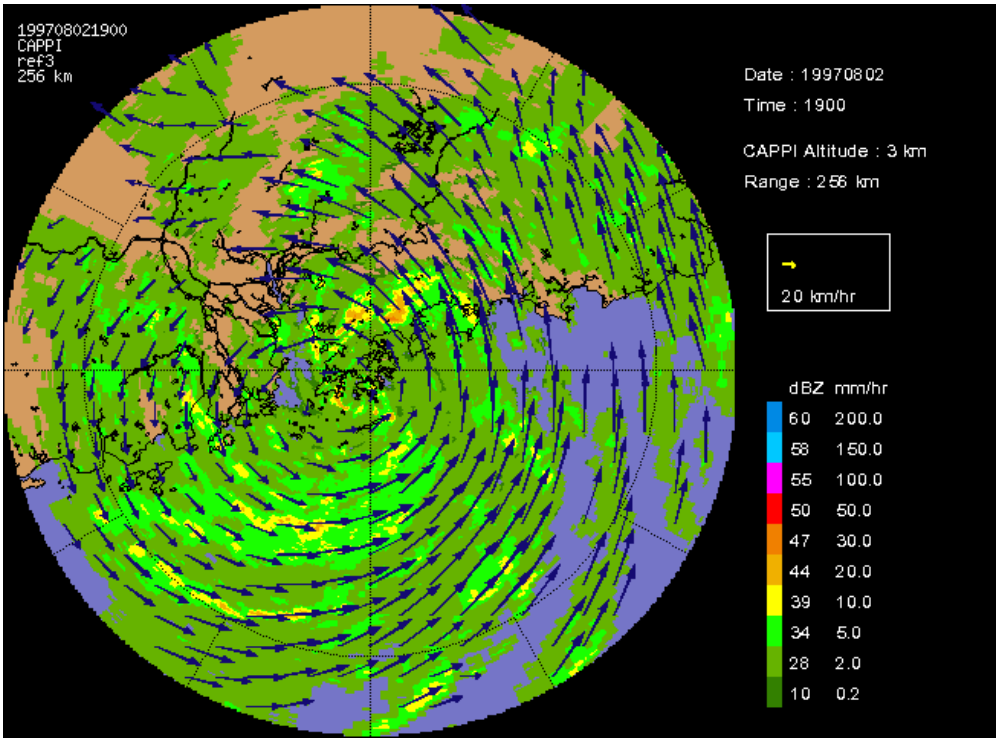

Figure 3 TREC analysis of Typhoon Victor (9712) over Hong Kong at 19:00 HKT on 2 August 1997.

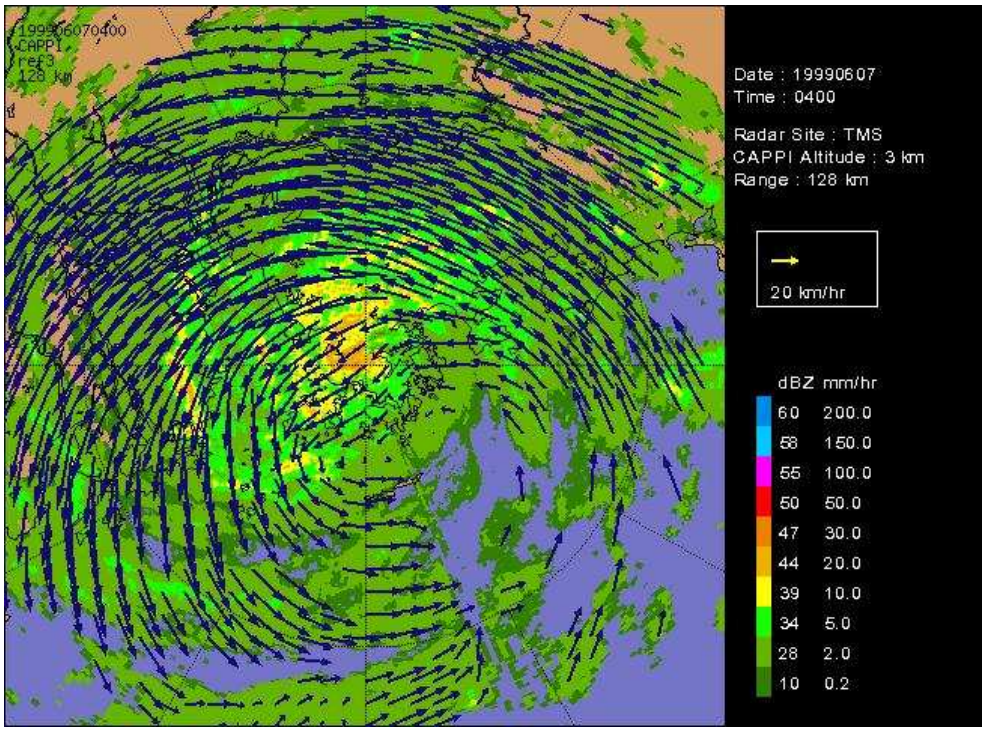

Figure 4 TREC analysis for Typhoon Maggie (9903) over Hong Kong at 4:00 HKT on 7 June 1999.

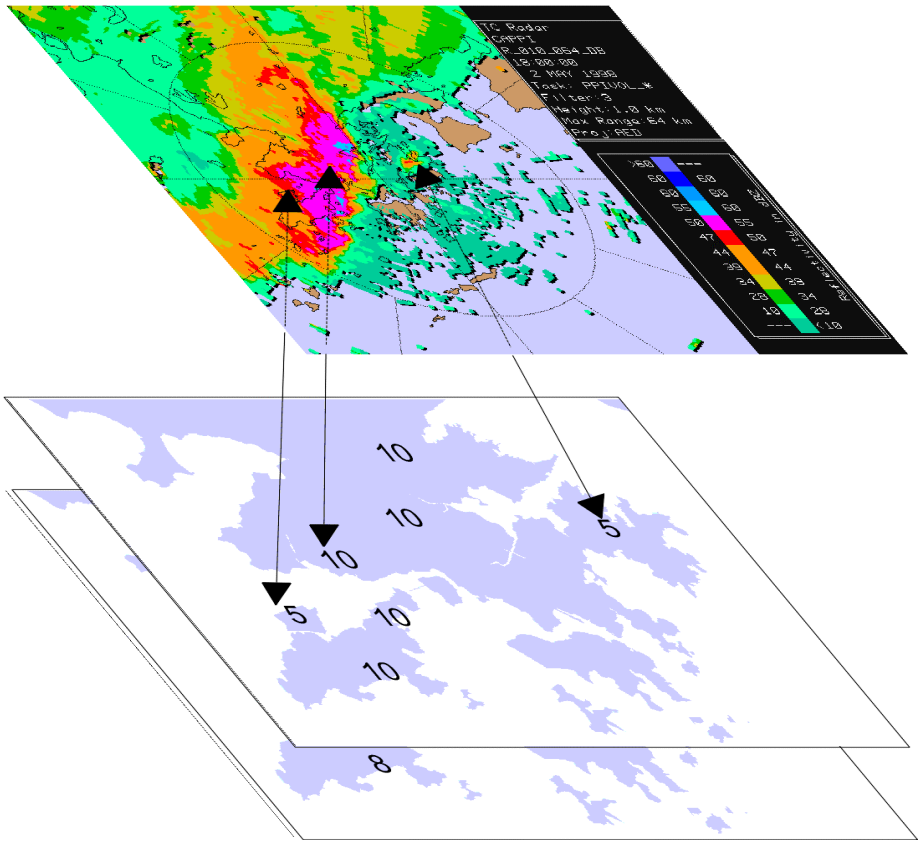

Figure 5 Schematic diagram showing the calibration of radar reflectivity using real-time raingauge measurements.

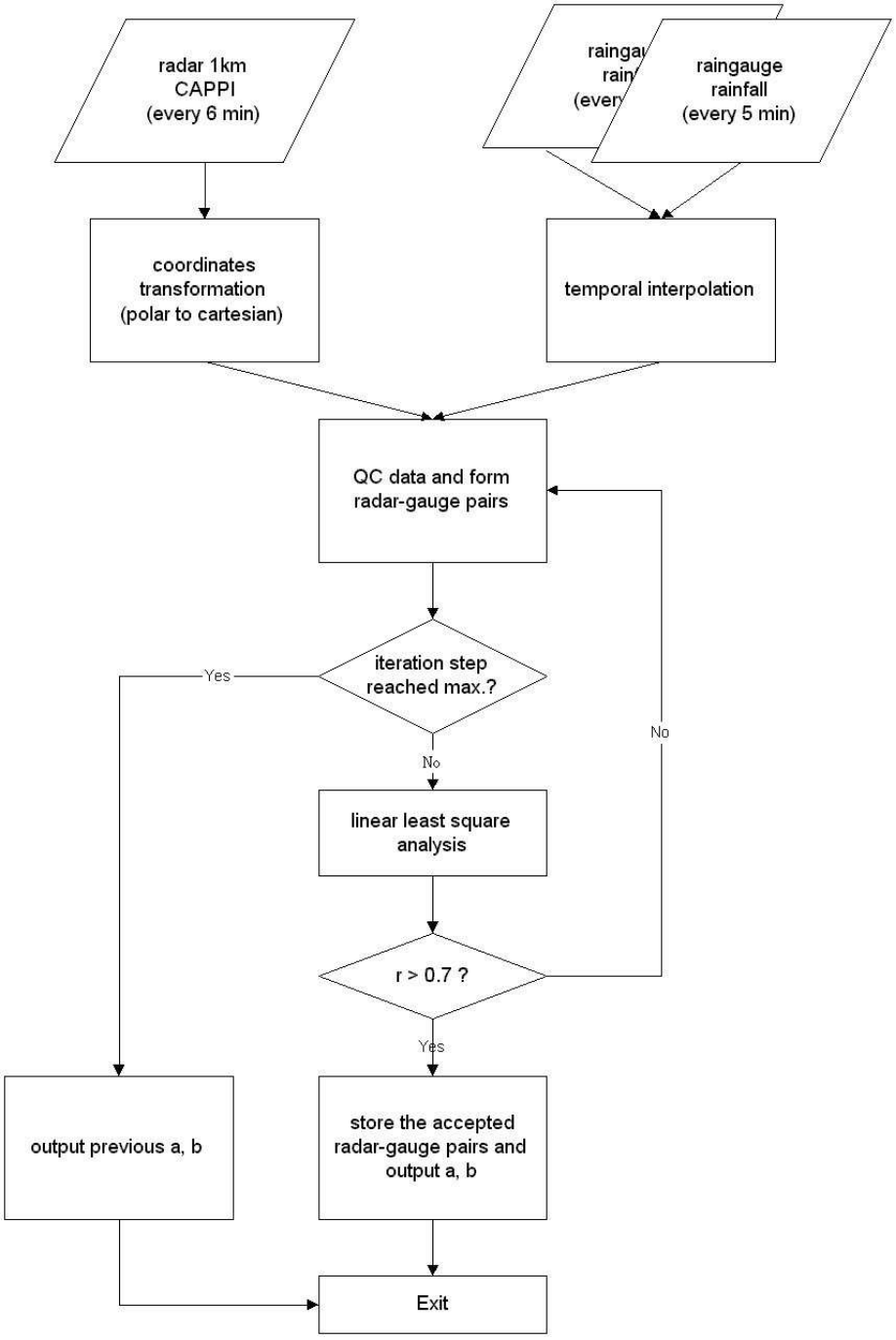

Figure 6 Flow diagram for the automatic radar-raingauge adjustment.

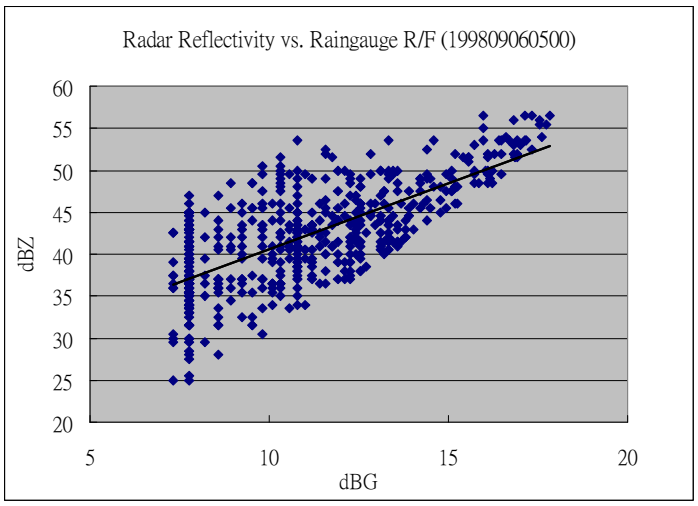

(a)

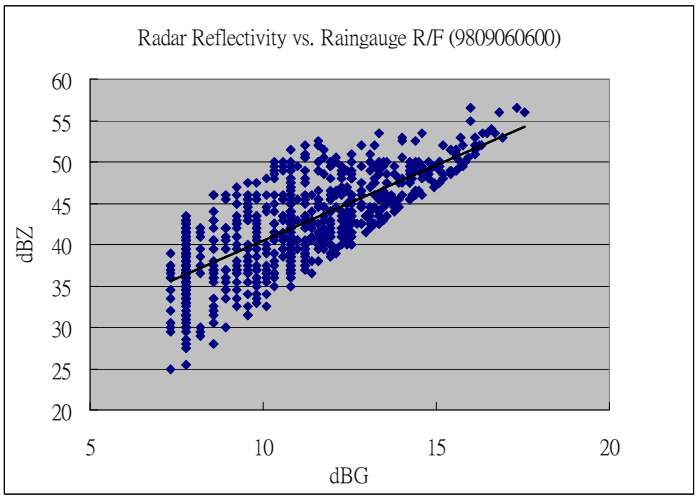

(b)

Figure 7 Scattered plots of radar-raingauge analysis for a rainstorm case on 9 June 1998. The parameters obtained from the least square analysis are: (a) at 5:00 HKT a=395, b=1.5, correlation coefficient=0.71; (b) at 6:00 HKT a=258, b=1.6, correlation coefficient=0.77.

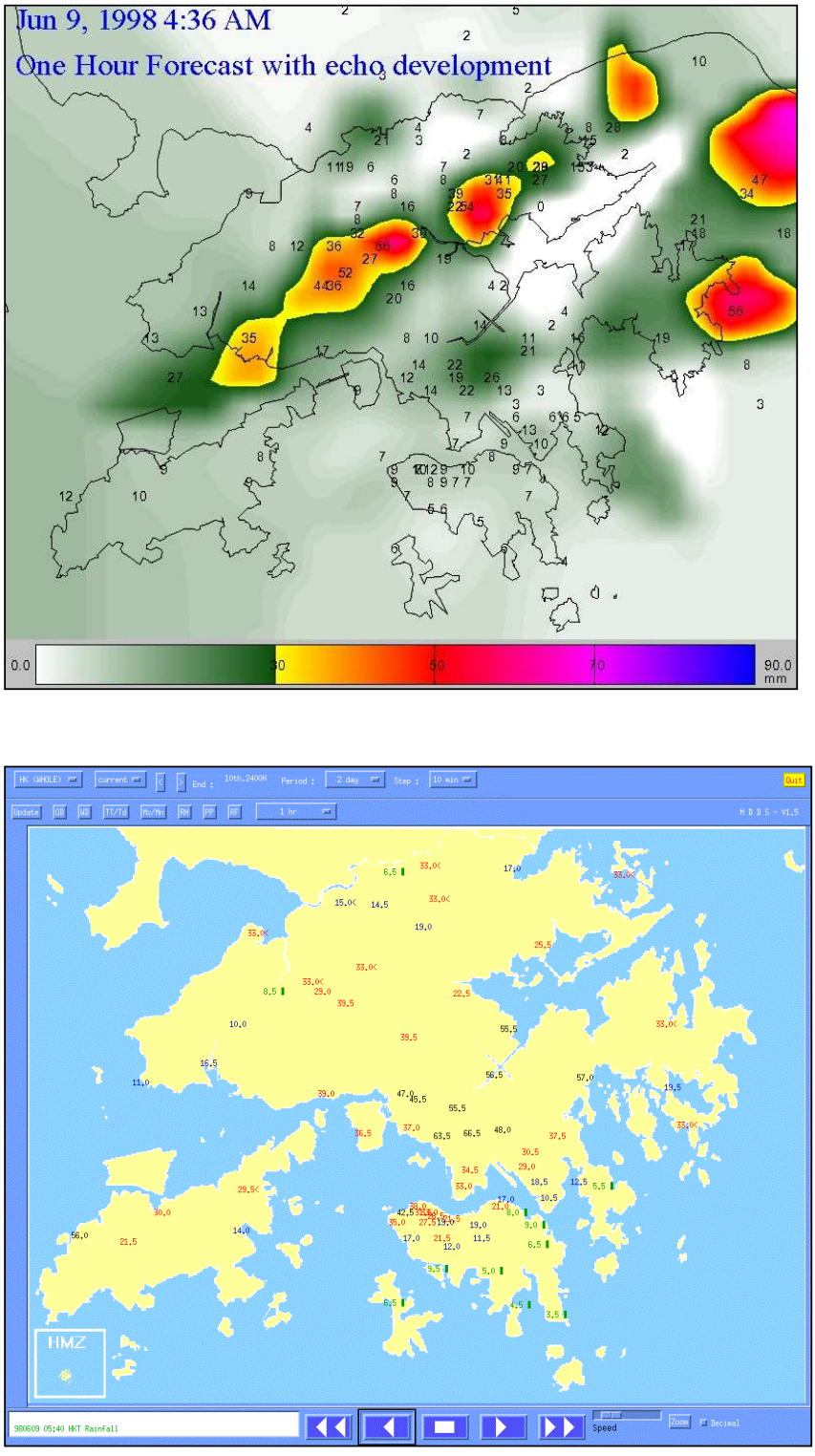

Figure 8 One hour rainfall forecast by SWIRLS issued at 4:36 HKT on 9 June 1998 (upper panel) and the corresponding one hour rainfall accumulation over the raingauges from 4:40 HKT to 5:40 HKT on 9 June 1998 (lower panel).

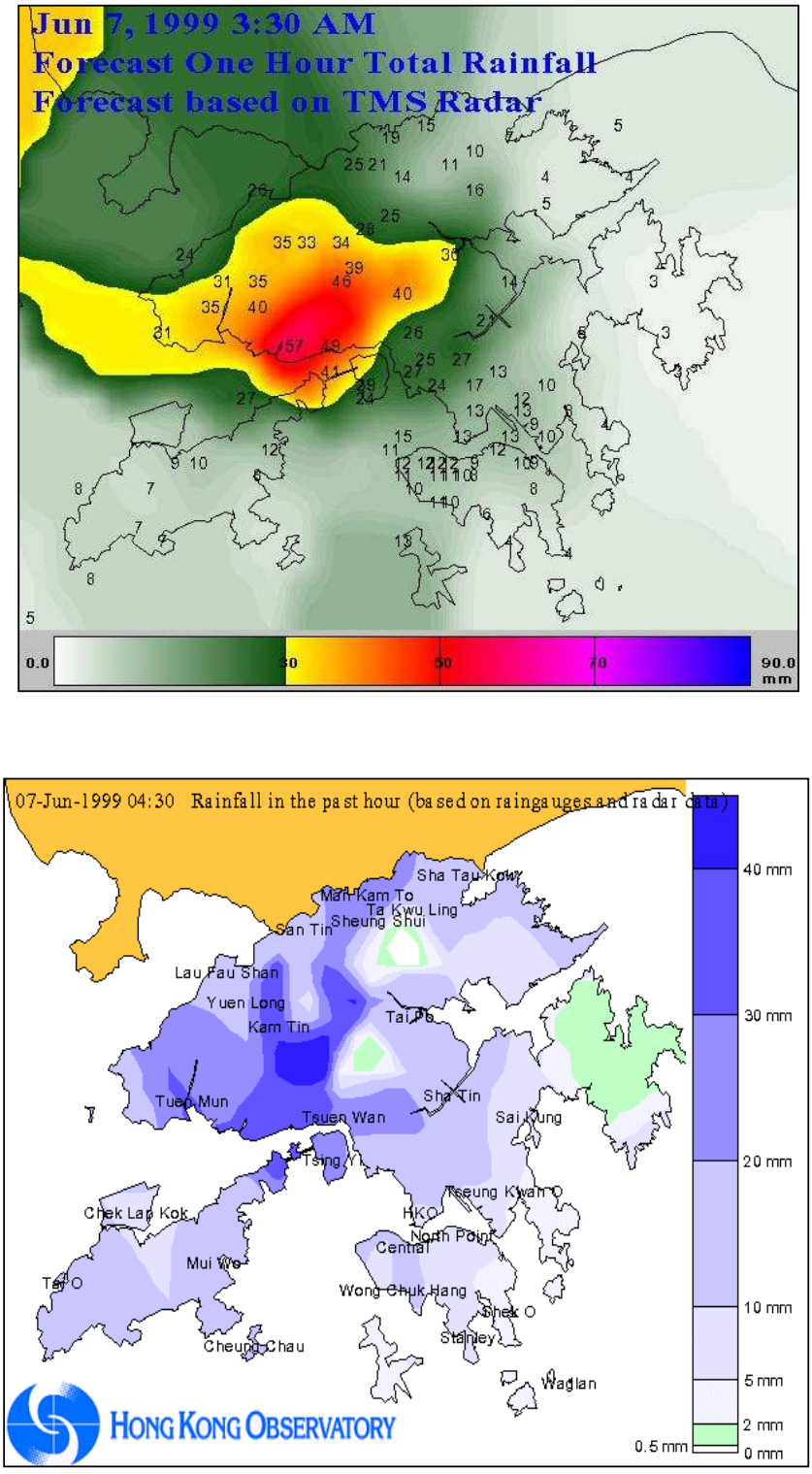

Figure 9 One hour rainfall forecast by SWIRLS for Typhoon Maggie issued at 3:30 HKT on 7 June 1999 (upper panel) and the corresponding one hour rainfall accumulation reported by the raingauges from 3:30 HKT to 4:30 HKT on 7 June 1999 (lower panel).

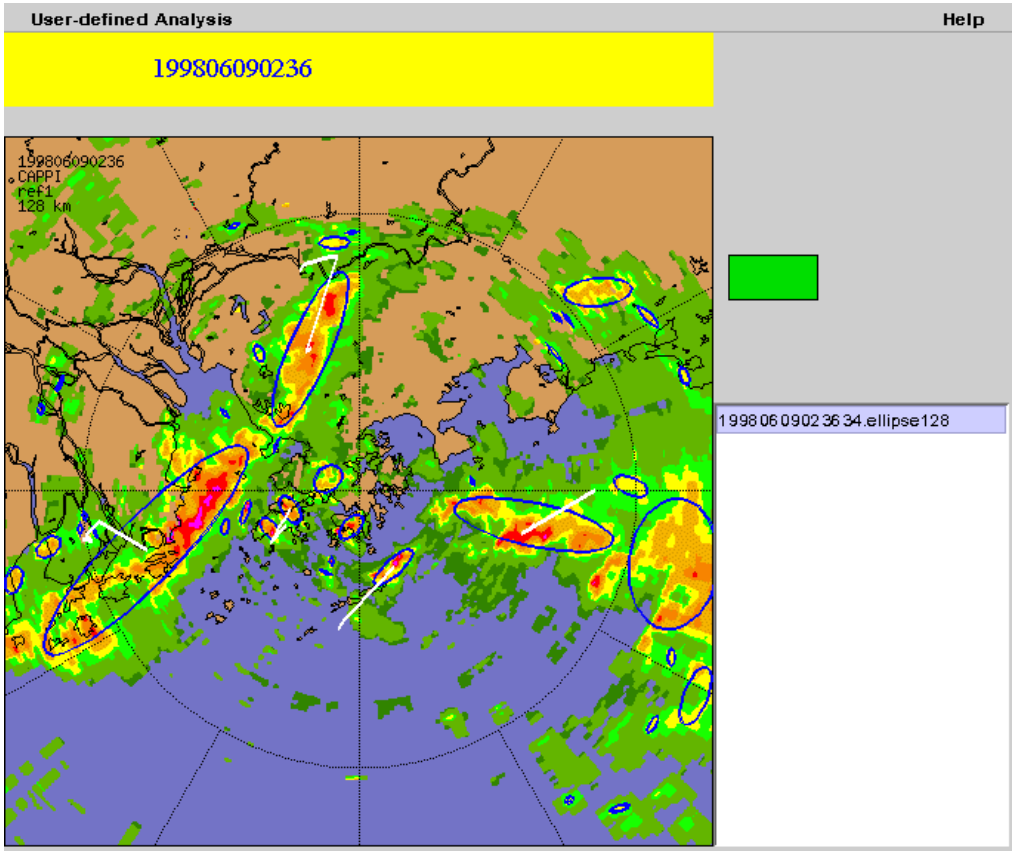

Figure 10 Complex interaction of echo groups on 9 June 1998 as revealed by the GTREC analysis. White lines connecting to centroids of ellipses indicate movement history of echo groups. One possible interpretation is that the SW-NE orientated squall line was moving southeastwards towards a slow-moving converging echo line lying just off the coast to the east of Hong Kong.

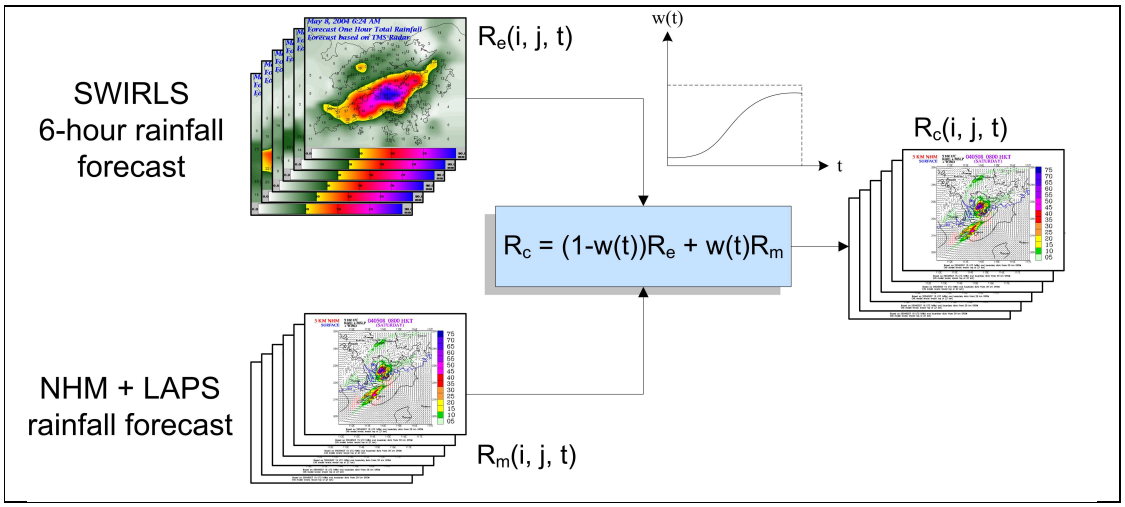

Figure 11 Schematic diagram showing the components in RAPIDS

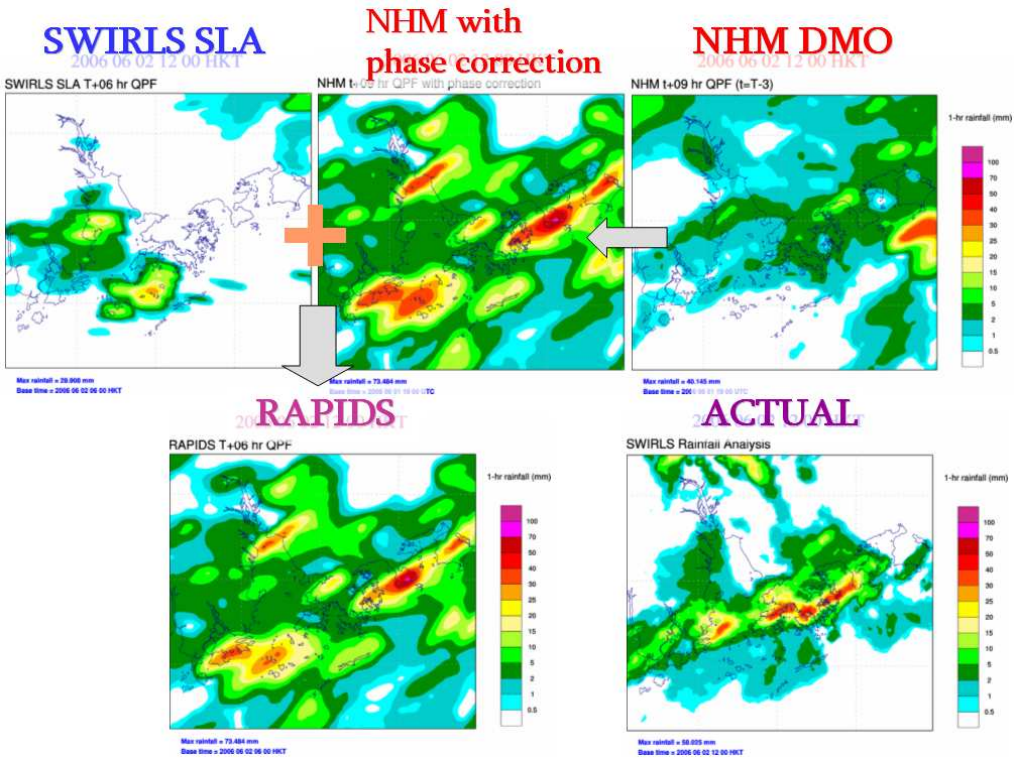

Figure 12 RAPIDS 6-hr forecast valid at 12 HKT 2 June 2006. Forecast from NHM (NHM DMO) is adjusted according to phase correction parameters calculated at 06 HKT. The corrected NHM QPF is added to SWIRLS forecast according weighting specified by the curve shown in Fig. 13 to form the RAPIDS QPF. Actual rainfall analysis at 12 HKT is shown in lower-right panel.

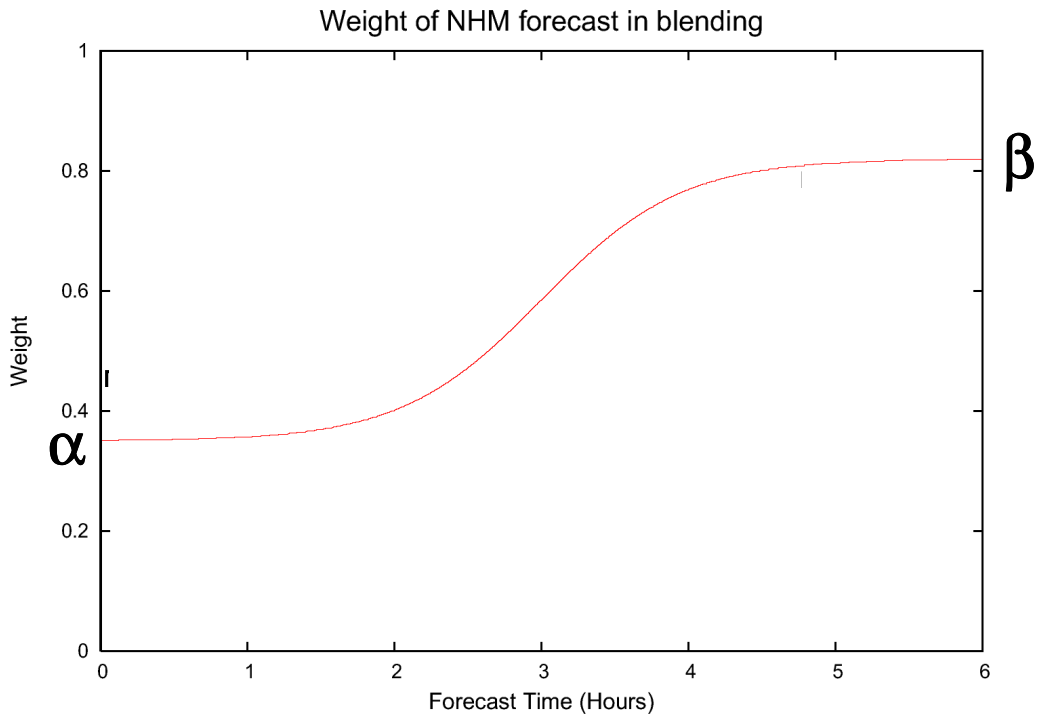

Figure 13 Weighting of NHM QPF for blending within the 6-hour forecast time window.

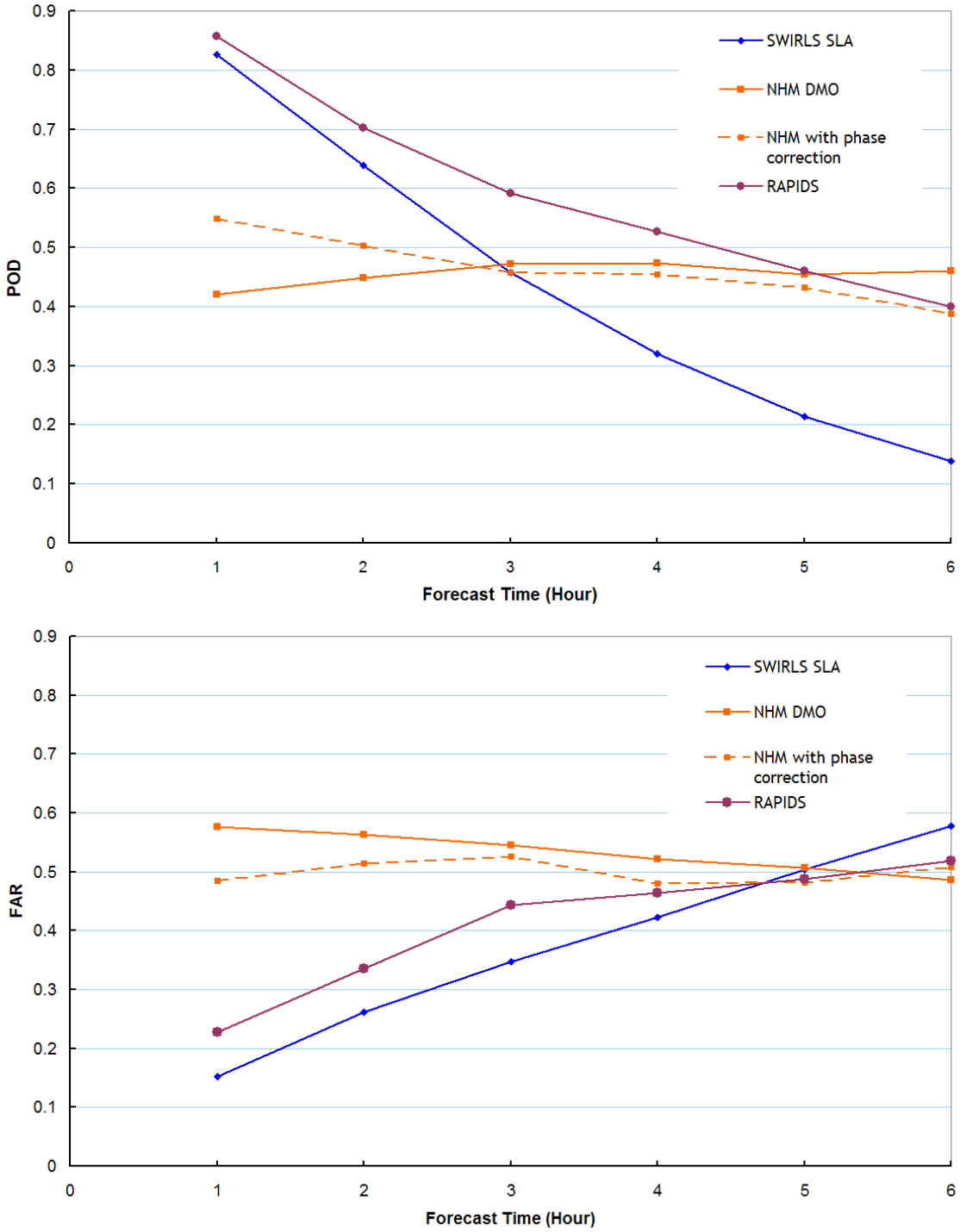

Figure 14 POD (upper) and FAR (lower) showing the verification statistics of QPF from: (i) SWIRLS SLA (blue line with diamonds), (ii) NHM DMO (orange line with squares), (iii) NHM with phase correction (dashed orange line with squares), and (iv) RAPIDS (purple line with circles). A homogeneous set of cases in 2005 (167 cases in total) are used for validating the four types of QPF products.